The International Journal of Cardiovascular Imaging (2019) 35:1701–1707
https://doi.org/10.1007/s10554-019-01596-8

ORIGINAL PAPER

CT-derived left ventricular global strain: a head-to-head comparison with speckle tracking echocardiography

F. Ammon[1] · D. Bittner[1] · M. Hell[1] · H. Mansour[2] · S. Achenbach[1] · M. Arnold[1] · M. Marwan[1]

Received: 9 December 2018 / Accepted: 1 April 2019 / Published online: 5 April 2019

Abstract

We assessed CT-derived left ventricular strain in a cohort of patients referred for transcatheter aortic valve implantation (TAVI) and validated it against 2 dimensional speckle tracking echocardiography as the gold standard. 65 consecutive patients with symptomatic aortic valve stenosis referred for CT imaging prior to TAVI were included in this analysis. For all patients, retrospectively ECG-gated multi-phase functional CT data sets acquired with identical reconstruction parameters were available. All data sets were acquired using a third generation dual source system. In all patients, multiphase reconstructions in increments of 10% of the cardiac cycle were rendered (slice thickness 0.75, increment 0.5 mm, medium smooth reconstruction kernel) and transferred to a dedicated workstation (Ziostation2, Ziosoft Inc., Tokyo, Japan). Additional functional reconstructions for dynamic assessment and quantification of strain were processed. Multiplanar reconstructions (MPR) of the left ventricle similar to standard echocardiographic 4, 2 and apical 3 chamber views were rendered in CT. Similar to echocardiographic longitudinal strain, the perimeter of the left ventricle was manually traced within the myocardium and peak maximal shortening as a parameter representing longitudinal strain was calculated for each view and averaged to obtain a marker for global longitudinal strain (CT perimeter-derived strain). Furthermore, for quantification of 3-dimensional strain, endocardial and epicardial borders of myocardium were marked in six short axis views and peak maximum 3- dimensional strain of the myocardium was calculated in standard six basal, six mid and four apical segments. 3-dimensional strain values of the 16 standard segments as well as perimeter-derived strain values in the three standard windows were averaged to obtain global strain. Echocardiography was performed in all patients before CT data acquisition. Digital loops were acquired from three apical views (four-, two-, and three chamber views). For assessment of 2 dimensional global longitudinal strain (GLS), recordings were processed with acoustic-tracking software allowing offline semiautomated speckle-based strain analyses. The mean age of all 65 patients was 81 ± 5 years. The mean echocardiographic ejection fraction and mean echocardiographic GLS were 50 ± 12% and −13.6 ± 4.5%, respectively. The mean CT-derived peak 3-dimensional global strain and mean peak strain derived by perimeter was 43.2 ± 13.5% and −11.2 ± 3.5%, respectively. Both CTderived global 3D-strain and perimeter derived strain showed a significant correlation to GLS derived by echocardiography ($r = -0.8$, $p < 0.0001$ for 3D strain and $r = 0.71$, $p < 0.0001$ for perimeter-derived strain). Bland-Altman analysis showed a systematic underestimation (i. e. worse strain values) of CT perimeter-derived strain compared to GLS by echocardiography (mean difference −2.4% with 95% limits of agreement between 4% to −9%). ROC Curve analysis assuming a normal GLS when less than −18% showed that a CT-derived peak 3-dimensional global strain cut-off-value of 45% has a sensitivity of 91% and a specificity of 60% for detecting normal left ventricular strain (AUC 0.81, $p = 0.001$). For CT perimeter-derived strain, a cut-off value of −12%—assuming a normal echocardiographic GLS when less than −18%—achieved a sensitivity of 82% and a specificity of 61% (AUC of 0.82, $p = 0.001$) for detecting abnormal left ventricular strain. Using dedicated software, assessment of CT-derived left ventricular strain is feasible and comparable to strain derived by echocardiographic 2 dimensional speckle tracking.

Keywords Left ventricular global strain · Speckle tracking · Cardiac CT angiography · Echocardiography

✉ F. Ammon
fabian.ammon@uk-erlangen.de

Extended author information available on the last page of the article

Introduction

Speckle tracking echocardiography is a well-established tool for assessing myocardial deformation. Many reports have demonstrated the usefulness of global longitudinal strain measurements in various clinical settings—e.g. determination of timing for mitral valve surgery in severe regurgitation as well as prediction of cardiovascular events and adverse outcomes in chronic heart failure patients. [1–5].

Nevertheless, an important prerequisite for 2-dimensional speckle tracking echocardiography is good image quality. To determine global longitudinal strain, high-quality acquisitions of apical four-, two- and three-chamber views without foreshortening of the left ventricle are necessary. An artifact-free ECG signal is required and breathing artifacts need to be avoided. [6] Moreover, acoustic shadowing, limited planes and patient-specific conditions are—among others—reasons for insufficient image quality especially in the elderly population. [7, 8] In fact, in a cohort of 559 consecutive patients examined by Benyounes et al. for the feasibility of strain imaging to predict reduced left ventricular function in clinical routine, 9.1% of the transthoracic echocardiographic studies were not suitable for strain analysis either due to impaired image quality or to rhythm disturbances. [9].

ECG-gated CT angiography is an established diagnostic tool for the evaluation of coronary artery disease. Multiple studies have also shown its usefulness to determine cardiac dimensions and left ventricular ejection fraction. [10].

Recently, several studies have reported the potential assessment of left ventricular strain using cross-sectional imaging modalities such as CT and magnetic resonance. [11–13] So far, a head-to-head comparison of echocardiographic 2-dimensional longitudinal strain—the most frequently used strain measure in clinical routine—with CT derived strain has not been reported.

The aim of this study was to assess CT-derived left ventricular strain in a cohort of patients referred for transcatheter aortic valve implantation (TAVI) and to validate it against 2-dimensional speckle tracking echocardiography as the gold standard.

Materials and methods

Study design and patient population

This is a single-center, retrospective analysis. 140 consecutive patients with high grade aortic valve stenosis referred for CT imaging prior to TAVI were scanned for inclusion in this study. Out of these, 67 patients with reduced echocardiographic image quality not allowing for strain analysis in all myocardial segments were excluded. Furthermore, eight patients with CT data not covering the entire myocardium were further excluded from analysis. Finally 65 patients were included in this study. CT exams had been performed as a part of routine imaging for planning the TAVI procedure.

DSCT data acquisition and image reconstruction

Pre-interventional CT was performed using a third generation dual source CT system (Somatom Force, Siemens Healthineers, Forchheim, Germany). Retrospectively ECG-triggered spiral acquisition was performed in all patients. The scan range extended from the proximal ascending aorta to the caudal aspect of the heart. The following scan parameters were used: tube voltage 100 kV, tube current time product 500 mAs, 0.6 mm collimation, 250 ms rotation time. ECG-correlated tube current modulation was used and full radiation exposure was set between 10–70% of the R-wave to R-wave interval, while tube current was reduced to 20% outside this window. Contrast agent transit time was determined by giving a bolus of 10 ml contrast agent (Ultravist 370®, Bayer vital, Leverkusen, Germany). Afterwards 50 ml of contrast agent at a flow rate of 5 ml/s, followed by 50 ml of saline flush at the same flow rate was injected for CT angiography.

For functional assessment of the left ventricle, a multiphase reconstruction at every 10% of the cardiac cycle was rendered using a small field of view (150 mm). All reconstructions were rendered using a medium soft convolution kernel (Siemens Bv40) with a slice thickness of 0.75 mm and slice increment of 0.5 mm. Iterative reconstruction (Admire®, Siemens Healthineers, Forchheim, Germany) at a strength level of two was used.

CT analysis of left ventricular strain

CT data sets were transferred to a dedicated workstation (Ziostation2, Ziosoft Inc., Tokyo, Japan) for processing to determine strain. To quantify left ventricular longitudinal strain, multiplanar reconstructions (MPR) of the left ventricle were manually rendered in CT, similar to standard echocardiographic apical four-chamber, two-chamber and three-chamber views. The perimeter of the left ventricle in all three views was manually traced within the midline of the myocardium—in a fashion similar to the determination of echocardiographic longitudinal strain—and peak shortening as a parameter representing longitudinal strain was calculated for each view (Fig. 1). Peak shortening in the three multiplanar reconstructions was averaged to obtain a

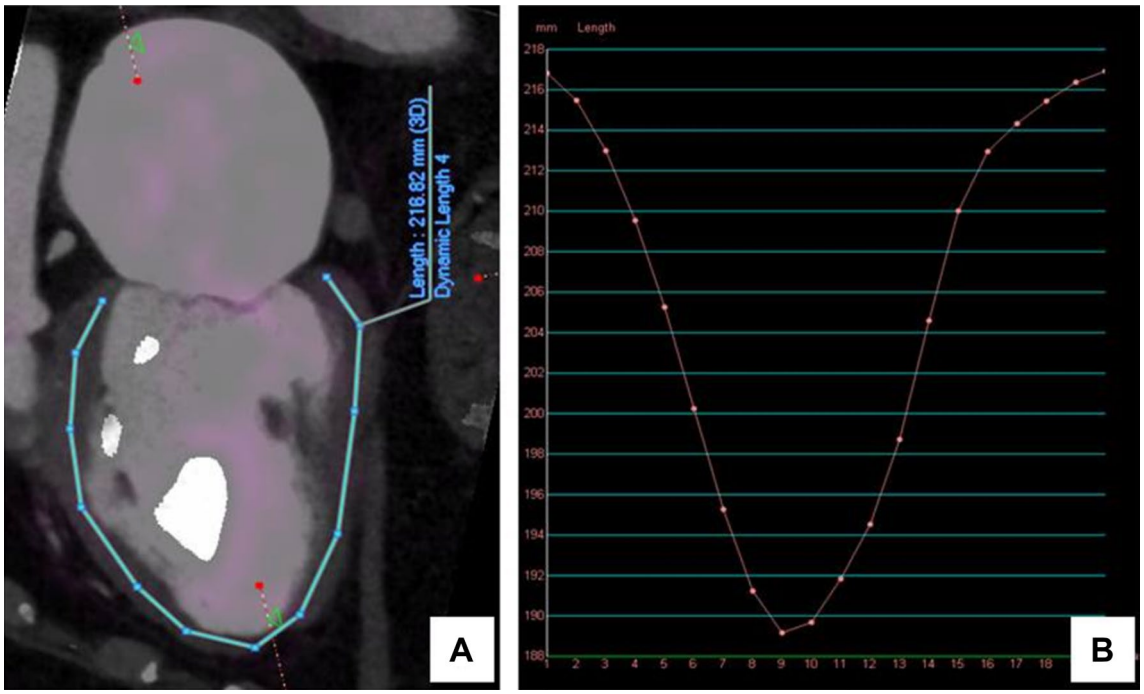

Fig. 1 **a** Multiplanar reconstruction of the left ventricle showing standard two-chamber view. The ventricle contours are traced (line). **b** Dynamic changes of ventricular length in two chamber view through the cardiac cycle as a surrogate of longitudinal strain are shown in this graph

measure of global longitudinal strain, named "CT perimeter-derived strain".

The concept of maximum principal strain (3-dimensional strain) to assess myocardial strain allows to represent the maximum tensile strain at any given point. To obtain maximum principal strain, the motion coherent algorithm was first applied to the original 10% increment data to generate the interphase CT images from two neighboring phases. In this way, interpolated data at 5% increments was obtained in order to reduce noise to improve motion coherence. [14] By image matching and model matching algorithms on the interpolated data the matrix of motion vectors was generated. [15] Based on the matrix of motion vectors, the maximum principal strain was calculated based on expansion of the principal direction from the starting point to any points on each phase during the cardiac cycle. [11].

For quantification of 3-dimensional strain, data sets along with additionally reconstructed strain data sets were merged by the dedicated strain-analysis software. First, the tips of the mitral valve and the apex of the left ventricle were manually determined in four-chamber and two-chamber views. Endocardial and epicardial borders of myocardium were automatically marked by the software in six short axis views from basal to apical and manual correction was done when necessary. The maximum 3-dimentional strain of the whole myocardium was then automatically calculated by the dedicated software in standard six (anterior, anterolateral, inferolateral, inferior, inferoseptal, anteroseptal) basal and mid segments and four (anterior, lateral, inferior, septal) apical segments (Fig. 2). Strain values of the 16 segments were averaged to obtain global maximum principal strain.

Echocardiographic analysis of left ventricular strain

ECG-gated echocardiography was performed in all included patients before CT data acquisition. 2-dimensional echocardiographic studies were performed with a Vivid 7 system (General Electric Medical Systems, Milwaukee, WI, USA). Digital loops were acquired from three apical views (four-, two-, and three-chamber views). For assessment of 2-dimensional global longitudinal strain (GLS), recordings were processed with acoustic-tracking software (EchoPAC BT12; GE Medical Systems, Milwaukee, WI) allowing offline semi-automated speckle-based strain analyses. Ejection fraction was quantified by visual estimation.

Statistical analyses

The Kolmogorov–Smirnov test was used to test for normal distribution. Normally distributed data are presented as mean ± standard deviation. Mean values were compared using a two-sided paired *t* test in normally distributed data and Mann–Whitney test for non-parametric data. Results were deemed significant when the p value was < 0.05. ROC curve analyses were performed to identify CT strain values with the best diagnostic performance compared to

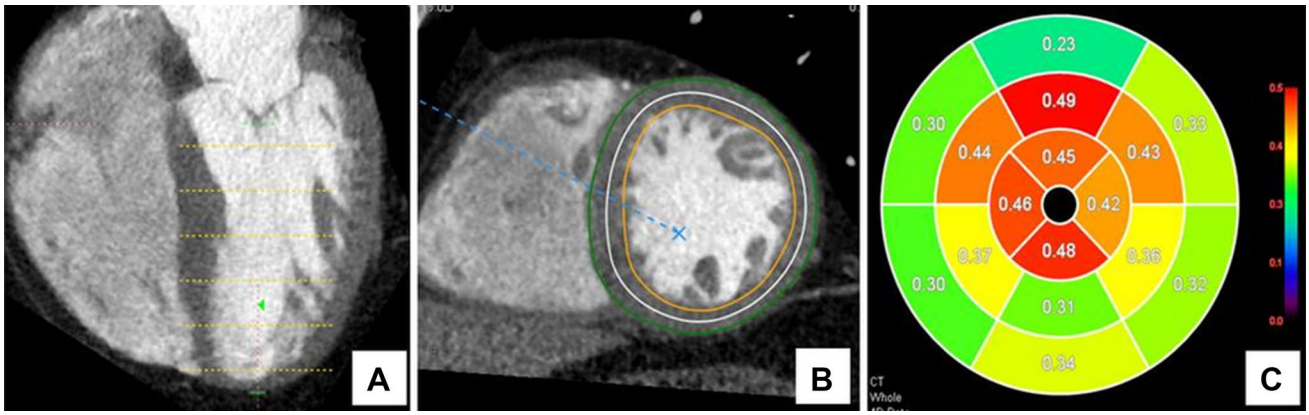

Fig. 2 Assessment of three-dimensional strain in CT. **a** Multiplanar reconstruction of the left ventricle in standard four-chamber-view. The dotted lines mark the left ventricle from the tip of the mitral valve to the apex. **b** Automatic detection of the epicardial and endocardial contours by the software. **c** Bulls-eye demonstration of left ventricular strain of 16 myocardial segments. Eg. 0.49 is equivalent to a strain value of 49%

Table 1 Patients' data

	Patients (n = 65)
Age (years)	81 ± 5
Male sex	33/65
Ejection fraction (mean ± SD)	50 ± 12%
Echocardiographic GLS (mean ± SD)	−13.6 ± 4.5%
CT perimeter strain (mean ± SD)	−11.2 ± 3.5%
3D CT global strain (mean ± SD)	43.2 ± 13.5%
Diabetes mellitus	28%
Arterial hypertension	83%
Hyperlipidemia	34%
Atrial fibrillation	32%
Implanted PM or ICD	9%
Chronic kidney disease	43%
COPD	17%
Previous cardiac surgery	14%
Coronary artery disease	55%

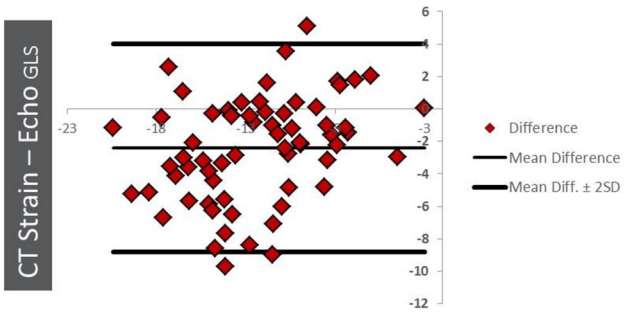

Fig. 3 Bland–Altman-Plot of CT perimeter-derived strain and echocardiographic global longitudinal strain showing a systematic underestimation of stain in CT. Mean difference −2.4%, 95% limits of agreement 4 to −9%

echocardiography as the gold standard. All statistical analyses were performed using IBM® (New York) SPSS® Statistics (version 21.0).

Results

65 patients with severe aortic stenosis were included in this analysis. Mean patient age was 81 ± 5 years, 33 patients were male (51%). Over 80% of patients received CT imaging on the same or the following day as echocardiography. Mean echocardiographic ejection fraction by visual estimate was 50 ± 12% and mean echocardiographic global longitudinal strain (GLS) was −13.6 ± 4.5%. Table 1 shows the baseline clinical characteristics of the patients.

After processing the strain and dynamic tracing data sets, analysis of CT-derived maximum principal strain as well as perimeter-derived strain required for each 5 min on average. Assessment of CT-derived strain was successfully performed in all patients.

The mean CT-derived peak global maximum principal strain (3D strain) and the mean peak strain derived by perimeter were 43.2% ± 13.5% and −11.2 ± 3.5%, respectively. Both CT-derived global 3D-strain and perimeter-derived strain showed a significant correlation to GLS derived by echocardiography ($r = -0.8$, $p < 0.0001$ for 3D strain and $r = 0.71$, $p < 0.0001$ for perimeter-derived strain, respectively). Bland–Altman analysis showed a systematic underestimation of CT perimeter-derived strain compared to GLS by echocardiography (mean difference −2.4% with 95% limits of agreement between 4 and −9%) (Fig. 3).

11 patients had an echocardiographic GLS of < – 18%. ROC Curve analysis assuming a normal echocardiographic GLS when < – 18% [16, 17], showed that a CT-derived 3D strain cut-off value of 45% has a sensitivity of 91% and a specificity of 60% for detecting normal left ventricular strain (AUC 0.81, p = 0.001) (Fig. 4). For CT perimeter-derived strain, a cut-off value of – 12%—assuming a normal echocardiographic GLS when < – 18%—achieved a sensitivity of 82% and a specificity of 61% (AUC of 0.82, p = 0.001) for detecting abnormal left ventricular strain (Fig. 5).

Discussion

In this proof-of-concept study performed in a cohort of 65 patients with severe aortic valve stenosis, assessment of left ventricular strain from multi-phase CT data sets was shown to be comparable to standard clinical echocardiographic global longitudinal strain assessment. While measurement principles are slightly different and mean values are not identical, close correlation and a high area under the ROC curve was found for CT-derived strain compared to GLS in echocardiography.

Echocardiographic global longitudinal strain is a sensitive parameter of left ventricular function and deformation. Using speckle tracking, the maximum difference in the length of each myocardial segment during the cardiac cycle is compared to the primary length. The average change presented in percentage for all myocardial segments—physiologically a negative value because of shortening of the left ventricle during systole—is named global longitudinal strain [18–20].

CT-derived perimeter strain has a similar approach by referring the change of perimeter length in three apical views to the primary perimeter length at the beginning of cardiac contraction. Similar to echocardiographic global longitudinal strain, it has physiologically negative values. In our study, we could demonstrate a good correlation between both modalities (r = 0.71, p < 0.0001). However,—compared to echocardiographic GLS—CT-derived perimeter strain demonstrated systematically lower strain values on Bland–Altman analysis. These differences could be explained by inherent difference between both modalities.

Furthermore, three-dimensional CT assessment of LV strain has a different way of calculating left ventricular deformation. After defining the myocardium by marking endocardial and epicardial contours, a motion vector of every point in space can be calculated. The growth of length of the motion vector divided by its initial length gives a parameter of myocardial deformation. By dividing the myocardium in different segments—like standard echocardiographic segments—a parameter of strain for each segment

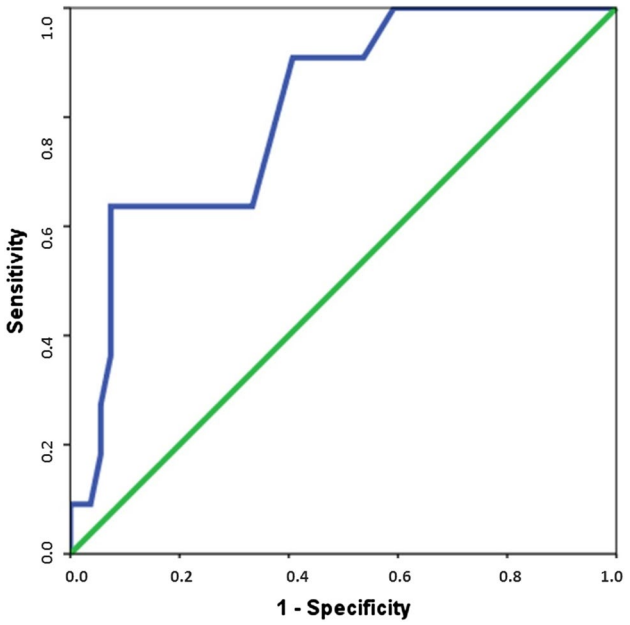

Fig. 4 ROC Curve analysis for diagnostic accuracy of three-dimensional CT strain for detecting normal echocardiographic normal GLS. Assuming a normal echocardiographic GLS when < – 18%, showed that a CT-derived 3D strain cut-off value of 45% has a sensitivity of 91% and a specificity of 60% for detecting normal left ventricular strain (AUC 0.81, p = 0.001)

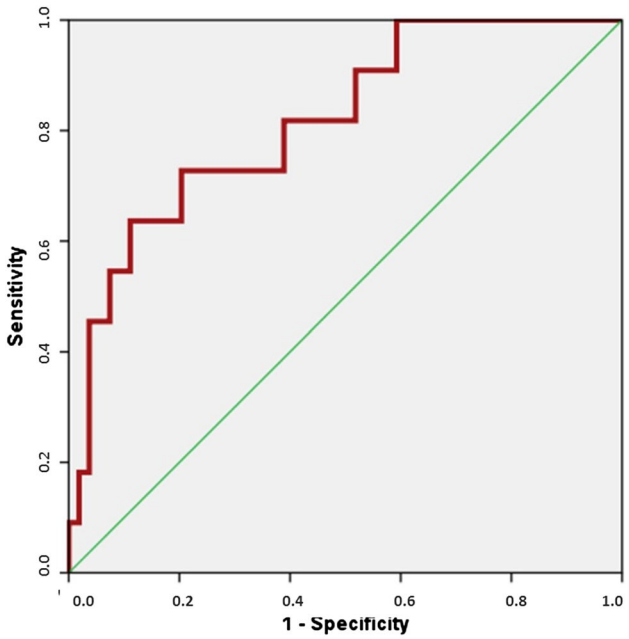

Fig. 5 ROC Curve analysis for diagnostic accuracy of CT perimeter-derived strain for detecting normal echocardiographic normal GLS. A cut-off value of CT perimeter-derived strain of – 12%—assuming a normal echocardiographic GLS when < – 18%—achieved a sensitivity of 82% and a specificity of 61% (AUC of 0.82, p = 0.001) for detecting normal left ventricular strain

is calculated. The average value of all segments for each phase of the cardiac cycle is calculated and the maximum difference during the cardiac cycle is considered as a 3D parameter of strain. As the name suggests, 3D CT strain does not only incorporate the longitudinal fraction of myocardial deformation, but also the radial and circumferential strain fraction alike. Unlike echocardiographic GLS and CT-derived perimeter strain, 3D CT strain has a positive value, and a high percentage suggests more deformation. In our cohort, a 3D strain value of 45% could be shown on ROC-curve analysis to detect normal echocardiographic GLS with a sensitivity of 91% and a specificity of 60%.

Recently, in a study by Tee et al., CT strain parameters using multimodality tissue tracking showed good correlation with radial and circumferential echocardiographic strain in a swine model. [21] Moreover, Tavakoli et al. used a motion detection algorithm to gain CT strain values. In their analysis, a good correlation of radial and circumferential strain with strain parameters acquired by echocardiography or MRI in a group of patients with ischemic heart disease, coronary artery disease, dilated cardiomyopathy as well as healthy volunteers could be demonstrated. [13] In a small cohort examined by Helle-Valle et al. radial CT strain showed excellent results in detecting infarcted myocardium owing to its high spatial resolution and high signal to noise ratio. It furthermore showed a good correlation with MR strain [22].

Several limitations need to be acknowledged for this study. Apart from the relatively small sample size, we included a cohort of patients with severe aortic stenosis referred for CT assessment prior to transcatheter valve replacement as for those patients full cycle CT acquisitions are performed per standard institution protocol and a wide range of strain values are expected. Hence, we cannot determine how CT-derived strain would perform in other populations or in a normal cohort. A large number of patients had to be excluded from this analysis if echocardiographic strain analysis could not be performed on all myocardial segments since, for reasons of comparisons to CT, assessment of the entire ventricle was necessary. Furthermore, normal reference values for CT-derived strain are not known and need to be compared to reference modalities in bigger cohorts. In our study, assuming normal left ventricular strain when echocardiographic 2-dimensional longitudinal strain was $< -18\%$, a cut-off-value of 45% for CT-derived 3D global strain had a sensitivity of 91% and a specificity of 60% for detecting normal ventricular strain. CT-derived perimeter strain demonstrated a comparable diagnostic performance (cut-off of -12% CT-derived perimeter strain showed a sensitivity of 82% and a specificity of 61% for detecting normal ventricular strain). Though the number of patients in our study with normal GLS was low (11/65)—all patients had severe aortic stenosis, known to often affect global longitudinal strain—, the cut-off-values of 45% of CT-derived 3D global strain or – 12% CT-derived perimeter strain can be a first step towards defining normal values. [23, 24] Lastly, for the purpose of CT assessment of strain, multiphase reconstructions are necessary that are associated with higher radiation exposure than most commonly used CT acquisition protocols. Echocardiography clearly has the advantage of the ease of performance and wide availability. Furthermore, no use of contrast agent and radiation is necessary and follow-up measurements are easier to achieve than with cardiac CT. Clearly echocardiography provides a higher temporal resolution with a frame rate for assessment of left ventricular strain usually within the range of 40–80 images per second. Cardiac CT provide three dimensional coverage of the myocardium, however an inferior temporal resolution compared to echocardiography which is inherent to the modality (temporal resolution of the third generation dual source system is 66 ms).

However, to our knowledge this is the first study to compare a novel algorithm for three dimensional assessment of strain in CT with standard echocardiography speckle tracking. We could demonstrate that CT assessment of left ventricular strain in a patient cohort planned for interventional treatment of aortic valve stenosis is feasible using dedicated software and is comparable to the current clinical gold standard.

Acknowledgements We would like to express our sincere thanks to Mr. Tsuyoshi Nagata from Ziosoft for his help and assistance in the pre-processing and analysis of the strain data as well as his continuous support with data analysis.

Compliance with ethical standards

Conflict of interest Mohamed Marwan has received speaker honoraria from Siemens Healthineers and Edwards Lifesciences. Martin Arnold is a consultant for St. Jude Medical and Edwards Lifesciences. The other authors declare that they have no conflict of interest.

Ethical approval All procedures performed in studies involving human participants were in accordance with the ethical standards of the institutional research committee and with the 1964 Helsinki declaration and its later amendments or comparable ethical standards.

Informed consent Informed consent was obtained from all individual participants included in the study.

References

1. Iacoviello M, Puzzovivo A, Guida P, Forleo C, Monitillo F, Catanzaro R et al (2013) Independent role of left ventricular global longitudinal strain in predicting prognosis of chronic heart failure patients. Echocardiography 30(7):803–811
2. Mentias A, Naji P, Gillinov AM, Rodriguez LL, Reed G, Mihaljevic T et al (2016) Strain Echocardiography and Functional Capacity in Asymptomatic Primary Mitral Regurgitation With Preserved Ejection Fraction. J Am Coll Cardiol 68(18):1974–1986

3. Motoki H, Borowski AG, Shrestha K, Troughton RW, Tang WH, Thomas JD et al (2012) Incremental prognostic value of assessing left ventricular myocardial mechanics in patients with chronic systolic heart failure. J Am Coll Cardiol 60(20):2074–2081
4. Russo C, Jin Z, Elkind MS, Rundek T, Homma S, Sacco RL et al (2014) Prevalence and prognostic value of subclinical left ventricular systolic dysfunction by global longitudinal strain in a community-based cohort. Eur J Heart Fail 16(12):1301–1309
5. Zhang KW, French B, May Khan A, Plappert T, Fang JC, Sweitzer NK et al (2014) Strain improves risk prediction beyond ejection fraction in chronic systolic heart failure. J Am Heart Assoc 3(1):e000550
6. Bansal M, Kasliwal RR (2013) How do I do it? Speckle-tracking echocardiography. Indian Heart J 65(1):117–123
7. D'Ascenzi F, Cameli M, Iadanza A, Lisi M, Zaca V, Reccia R et al (2013) Improvement of left ventricular longitudinal systolic function after transcatheter aortic valve implantation: a speckle-tracking prospective study. Int J Cardiovasc Imaging 29(5):1007–1015
8. Spethmann S, Dreger H, Baldenhofer G, Stuer K, Saghabalyan D, Muller E et al (2013) Short-term effects of transcatheter aortic valve implantation on left atrial mechanics and left ventricular diastolic function. J Am Soc Echocardiogr 26(1):64–71
9. Benyounes N, Lang S, Soulat-Dufour L, Obadia M, Gout O, Chevalier G et al (2015) Can global longitudinal strain predict reduced left ventricular ejection fraction in daily echocardiographic practice? Arch Cardiovasc Dis 108(1):50–56
10. Yamamuro M, Tadamura E, Kubo S, Toyoda H, Nishina T, Ohba M et al (2005) Cardiac functional analysis with multi-detector row CT and segmental reconstruction algorithm: comparison with echocardiography, SPECT, and MR imaging. Radiology 234(2):381–390
11. Marwan M, Ammon F, Bittner D, Rother J, Mekkhala N, Hell M et al (2018) CT-derived left ventricular global strain in aortic valve stenosis patients: a comparative analysis pre and post transcatheter aortic valve implantation. J Cardiovasc Comput Tomogr 12(3):240–244
12. Tavakoli V, Sahba N (2014) Assessment of subendocardial vs. subepicardial left ventricular twist using tagged MRI images. Cardiovasc Diagn Ther 4(2):56–63
13. Tavakoli V, Sahba N (2014) Cardiac motion and strain detection using 4D CT images: comparison with tagged MRI, and echocardiography. Int J Cardiovasc Imaging 30(1):175–184
14. Masri A, Schoenhagen P, Svensson L, Kapadia SR, Griffin BP, Tuzcu EM et al (2014) Dynamic characterization of aortic annulus geometry and morphology with multimodality imaging: predictive value for aortic regurgitation after transcatheter aortic valve replacement. J Thorac Cardiovasc Surg 147(6):1847–1854
15. Tanabe Y, Kido T, Kurata A, Sawada S, Suekuni H, Kido T et al (2017) Three-dimensional maximum principal strain using cardiac computed tomography for identification of myocardial infarction. Eur Radiol 27(4):1667–1675
16. Yingchoncharoen T, Agarwal S, Popovic ZB, Marwick TH (2013) Normal ranges of left ventricular strain: a meta-analysis. J Am Soc Echocardiogr 26(2):185–191
17. Marwick TH, Leano RL, Brown J, Sun JP, Hoffmann R, Lysyansky P et al (2009) Myocardial strain measurement with 2-dimensional speckle-tracking echocardiography: definition of normal range. JACC Cardiovasc Imaging 2(1):80–84
18. Blessberger H, Binder T (2010) NON-invasive imaging: two dimensional speckle tracking echocardiography: basic principles. Heart 96(9):716–722
19. Mor-Avi V, Lang RM, Badano LP, Belohlavek M, Cardim NM, Derumeaux G et al (2011) Current and evolving echocardiographic techniques for the quantitative evaluation of cardiac mechanics: aSE/EAE consensus statement on methodology and indications endorsed by the Japanese Society of Echocardiography. J Am Soc Echocardiogr 24(3):277–313
20. Sengupta PP, Krishnamoorthy VK, Korinek J, Narula J, Vannan MA, Lester SJ et al (2007) Left ventricular form and function revisited: applied translational science to cardiovascular ultrasound imaging. J Am Soc Echocardiogr 20(5):539–551
21. Tee MW, Won S, Raman FS, Yi C, Vigneault DM, Davies-Venn C et al (2015) Regional Strain Analysis with Multidetector CT in a Swine Cardiomyopathy Model: relationship to Cardiac MR Tagging and Myocardial Fibrosis. Radiology 277(1):88–94
22. Helle-Valle TM, Yu WC, Fernandes VR, Rosen BD, Lima JA (2010) Usefulness of radial strain mapping by multidetector computer tomography to quantify regional myocardial function in patients with healed myocardial infarction. Am J Cardiol 106(4):483–491
23. Miyazaki S, Daimon M, Miyazaki T, Onishi Y, Koiso Y, Nishizaki Y et al (2011) Global longitudinal strain in relation to the severity of aortic stenosis: a two-dimensional speckle-tracking study. Echocardiography 28(7):703–708
24. Ng ACT, Prihadi EA, Antoni ML, Bertini M, Ewe SH, Ajmone Marsan N et al (2017) Left ventricular global longitudinal strain is predictive of all-cause mortality independent of aortic stenosis severity and ejection fraction. Eur Heart J Cardiovasc Imaging 19(8):859–867

Affiliations

F. Ammon[1] · D. Bittner[1] · M. Hell[1] · H. Mansour[2] · S. Achenbach[1] · M. Arnold[1] · M. Marwan[1]

[1] Department of Cardiology, Friedrich-Alexander-Universität, Ulmenweg 18, 91054 Erlangen-Nürnberg, Germany

[2] Department of Cardiology, Ain Shams University Hospital, Cairo, Egypt